Catalysis Today 154 (2010) 13–20

Contents lists available at ScienceDirect

Catalysis Today

journal homepage: www.elsevier.com/locate/cattod

Gold, still a surprising catalyst: Selective hydrogenation of acetylene to ethylene over Au nanoparticles

Andreea C. Gluhoi[a,*], Johan W. Bakker[b,1], Bernard E. Nieuwenhuys[b,c]

[a] Avantium Technologies BV, Zekeringstraat 29, Amsterdam, The Netherlands
[b] Department of Heterogeneous Catalysis and Surface Chemistry, Leiden Institute of Chemistry, Leiden University, P.O. Box 9502, 2300 RA Leiden, The Netherlands
[c] Technische Universiteit Eindhoven, Postbus 513, 5600 MB Eindhoven, The Netherlands

ARTICLE INFO

Article history:
Available online 12 March 2010

Keywords:
Au catalysts
Acetylene hydrogenation
Ethylene hydrogenation
Polyethylene production
Selective hydrogenation of C_2H_2 in the presence of C_2H_4
Promoter
Deactivation
Ceria

ABSTRACT

The hydrogenation of C_2H_2 in the presence and the absence of C_2H_4 has been studied over un-promoted and promoted Au/Al_2O_3. A number of parameters have been varied: the Au particle size, the pre-treatment conditions (hydrogen versus oxygen) and the nature of the promoters. Promoters include ceria, lithium and barium oxides. Our results show that hydrogenation of C_2H_2 proceeds with 100% selectivity towards C_2H_4, both in the presence and the absence of C_2H_4. Moreover, there is a strong dependence of the catalytic performance on the size of the Au particles: Au particles below 3 nm enhance the C_2H_2 conversion both in the absence and the presence of C_2H_4, without decreasing the selectivity to C_2H_4. Furthermore, metallic Au and Ce^{4+} appear to be more effective than Au^{3+} and Ce^{3+}. Our findings also indicate that Li_2O has a beneficial effect on C_2H_2 conversion, while BaO has a slight detrimental effect, both having no influence on the selectivity to C_2H_4. The key to 100% selectivity to C_2H_4 resides in non-competitive adsorption of C_2H_2 and C_2H_4 on the Au surface when both hydrocarbons are present in the feed. The deactivation during C_2H_2 hydrogenation is a reversible process and is due to accumulation of C deposits on the catalyst surface, as result of C_2H_2 adsorption on different active Au sites. These deposits can be easily burned off by a thermal treatment in oxygen.

1. Introduction

The selective hydrogenation of acetylene is a very important catalytic process from an industrial point of view due to the large-scale production of polyethylene. A small quantity of acetylene (<3%) is present in the ethylene feedstock. Typically Pd-based catalysts are employed to eliminate these traces of acetylene from the ethylene streams [1–5]. High selectivity to ethylene and long-term catalyst stability are particularly desired for the selective acetylene hydrogenation process. However, since hydrogenation of acetylene is a series reactions with respect to the hydrocarbons (acetylene → ethylene → ethane) [6], and a parallel reaction with respect to hydrogen activation, the selectivity to ethylene decreases drastically with increasing acetylene conversion. In the case of Pd-based catalysts, it is generally accepted that the rate of the reaction is proportional to the available surface area of the active metal phase: smaller size (higher dispersion) is desirable for the Pd particles. The activity of the catalyst usually decays during the hydrogenation and this phenomenon is attributed to hydrocarbon build-up, also known as oligomers, which gradually cover the active surface of the metal particles. The oligomers formed during the acetylene hydrogenation process are a complex mixture of mainly unsaturated aliphatic hydrocarbons, which generally range from C_4 to C_{24} but can be as high as C_{60+}. The addition of promoters such as Ag, Co, Cu, Cr, alkali metals, lead acetate and metal oxides improves the selectivity of Pd-based catalysts to ethylene [6–8].

Other catalytic systems have also been studied for the hydrogenation of the acetylene. Gold is one of the most intriguing metal catalysts since it is only active if the particle size is in the nanometer range. Oxidation reactions over gold-based catalysts have been studied in more detail than hydrogenation reactions [9–12]. However, it is already known that for certain hydrogenation reactions Au-based catalysts display a surprisingly high selectivity to certain products, mainly because Au is able to selectively hydrogenate the C=O bond over the C=C bond [10,11]. A few studies have been reported concerning the hydrogenation of acetylene over various Au-based catalysts, both in batch [13] and flow reactors [14–18]. The Au-based catalysts that have been studied so far in the hydrogenation of acetylene were deposited on alumina [13], titania [15], silica [14,17] or ceria [16,18]. It has been reported that the selectivity to C_2H_4 is high in a certain temperature range. Some of the

* Corresponding author. Tel.: +31 20 586 8038.
E-mail address: gluhoi@chem.leidenuniv.nl (A.C. Gluhoi).
[1] Present address: NIMIC, Hosted by Interface Physics Group, Kamerlingh Onnes Laboratory, Leiden Institute of Physics, Leiden University, The Netherlands.

0920-5861/$ – see front matter © 2010 Elsevier B.V. All rights reserved.
doi:10.1016/j.cattod.2010.02.021

authors found that increasing the temperature above 200 °C has a negative effect on the selectivity towards ethylene [16,17]. It is, however, difficult to conclude which of the above mentioned supports are the best for Au-based catalysts because the reaction conditions were very different and the hydrogenation was sometimes performed under a large excess of hydrogen, which is known to increase the catalytic activity, but is not mimicking industrial conditions.

Surprisingly, no results have been reported regarding the catalytic performance of Au-based catalysts of the selective catalytic reduction (SCR) of the acetylene in the presence of ethylene, a process that would be highly valuable from an industrial point of view, especially when new catalytic systems with high selectivity and stability are developed.

The aim of this research was to follow the changes in the selectivity to C_2H_4 during C_2H_2 hydrogenation with:

- reaction temperature;
- additives;
- size of the Au particles;
- C_2H_4 addition;
- time on stream;
- pre-treatment conditions (hydrogen versus oxygen).

At first, the hydrogenation of C_2H_2 was studied in the absence of C_2H_4 over (un)promoted Au/Al_2O_3 (5wt% Au). Promoters include ceria, lithium oxide and barium oxide. We have been using the same promoters that in the past proved to enhance the catalytic performance of Au/Al_2O_3 in various oxidation reactions studied in our laboratory [19–25]. The second part of the study was dealing with the effect of ethylene addition on the C_2H_2 conversion and selectivity to various products.

An important issue found during SCR of C_2H_2 over Pd-based catalysts is the deactivation of the catalysts with the time on stream, mainly because of the build-up of the oligomers on the catalyst surface, which blocks the Pd active sites [7]. This issue has also been addressed with the Au-based catalysts tested in this study and the results are discussed in relation to the physico-chemical properties of the catalysts. The physico-chemical properties of the as-prepared Au-based catalysts have been assessed by a number of techniques such as: atomic absorption spectroscopy (AAS), BET surface area, X-ray diffraction (XRD), transmission electron microscopy (TEM) and temperature programmed desorption (TPD) and are correlated with the catalytic performance.

2. Experimental details

2.1. Catalyst preparation

We have already shown in several papers that homogeneous deposition precipitation (HDP) is a suitable method to prepare Au-based catalysts [19,20,23–25]: the gold deposition onto the support is high, the gold is not buried within the support, and a narrow particle size distribution is obtained.

The un-promoted gold-based catalysts (5 wt% Au) were prepared via HDP with urea, using $HAuCl_4{\cdot}3H_2O$ (Aldrich, 99.99%) as the gold precursor. Details concerning the preparation procedures have already been reported [20,22,24,25]. The freshly prepared Au/Al_2O_3 catalysts (i.e., after drying) were calcined in pure O_2 at 300 °C for 2 h.

The mixed supports in the form of $M^IO_x/(M^{II}O_x)/Al_2O_3$ (M^I, M^{II}: Ba, Li and Ce) were obtained via pore volume impregnation of γ-Al_2O_3 (Engelhard Al-4172P, S_{BET} = 275 $m^2\,g^{-1}$) with a solution of the corresponding nitrates. A detailed description of the experimental procedure can be found in [20]. Gold (5 wt%) was deposited onto $M^IO_x/(M^{II}O_x)/Al_2O_3$ ($M^I/M^{II}/Al$ = 1/(1)/15 by atomic ratio) using the same procedure as for the un-promoted Au/Al_2O_3. The catalysts were calcined in the same manner as the reference catalyst Au/Al_2O_3.

2.2. Catalyst characterization

The extent of gold deposition on the support was determined by means of atomic absorption spectroscopy (*AAS*). The samples were dissolved in aqua regia, filtrated and further diluted with distilled water prior to analysis. The results are summarized in Table 1.

BET surface areas of the catalysts were measured by N_2 physisorption at–196 °C using an automatic Qsurf M1 analyzer (Thermo Finnigan). Before each measurement the catalyst was degassed for 2 h at 200 °C in helium in order to remove the adsorbed impurities. For each measurement at least three points have been acquired in order to calculate the total surface area of the samples.

XRD measurements for the fresh catalysts were carried out using a Philips X'pert system with a PW3373/00 CuLFF DK180000 X-ray tube operated at 50 kV and 40 mA. The supports were also characterized by XRD in order to assess the crystalline phases of the various metal oxides added as additives and also to subtract their contribution before estimating the average Au particle size. The average gold particle size was estimated from XRD line broadening by using the Scherrer equation.

TEM measurements were performed using a JEOL 2010 microscope with a point-to-point resolution better than 0.2 nm. The sample was mounted on a carbon polymer supported copper microgrid. A few droplets of a suspension of the ground catalyst in isopropyl alcohol were placed on the grid, followed by drying under ambient conditions. The average gold particles and the particle size distribution were determined by counting at least 300 particles.

TPD measurements were performed on a similar system as the one used to test the catalytic performance of the Au-based catalysts (see below), but instead of a gas chromatograph (GC), a quadrupole mass spectrometer (Spectra Microvision Plus) was used to follow the effluent gas composition. Typically, 0.2 grams of catalyst were loaded in the reactor, followed by hydrogen reduction at 300 °C for 1 h. After cooling at room temperature, the sample was subjected to

Table 1
Catalyst characterization by means of AAS, BET, XRD and HRTEM.

Catalyst	Au (wt%)	S_{BET} ($m^2\,g^{-1}$)	$d_{Au}{}^a$ (nm)	$S_{Au}{}^a$ ($m^2\,g^{-1}$)	$d_{Au}{}^b$ (nm)	$S_{Au}{}^b$ ($m^2\,g^{-1}$)	D_{Au} (%)	$d_{Au}{}^c$ (nm)
Al_2O_3	-	275 ± 5	-	-	-	-	-	-
Au/Al_2O_3	4.1 ± 0.1	260 ± 5	4.3 ± 0.1	2.4 ± 0.1	5.2 ± 0.3	1.5 ± 0.3	11.5 ± 1.1	7.1 ± 0.1
$Au/Li_2O/Al_2O_3$	4.0 ± 0.3	278 ± 7	3.2 ± 0.1	3.0 ± 0.1	3.0 ± 0.1	2.5 ± 0.1	19.0 ± 1.0	6.4 ± 0.3
$Au/BaO/Al_2O_3$	3.6 ± 0.2	240 ± 8	<3.0	-	1.5 ± 0.2	6.2 ± 0.2	55.0 ± 1.2	7.4 ± 0.2
$Au/CeO_x/Al_2O_3$	4.5 ± 0.1	218 ± 11	<3.0	-	1.7 ± 0.2	7.1 ± 0.2	52.0 ± 1.3	7.8 ± 0.3
$Au/Li_2O/CeO_x/Al_2O_3$	4.6 ± 0.2	262 ± 10	<3.0	-	2.9 ± 0.1	3.8 ± 0.1	27.0 ± 5	7.7 ± 0.1
$Au/BaO/CeO_x/Al_2O_3$	4.4 ± 0.2	259 ± 7	<3.0	-	3.3 ± 0.1	3.0 ± 0.1	23.0 ± 5	8.1 ± 0.3

$d_{Au}{}^a$: mean diameter of gold particles, XRD, fresh catalysts (nm); $d_{Au}{}^b$: mean diameter of gold particles, HRTEM, fresh catalysts (nm); $d_{Au}{}^c$: mean diameter of gold particles, XRD, fresh catalysts thermally treated at 550 °C for 8 h (nm); $S_{Au}{}^a$: gold surface area, XRD ($m^2\,g^{-1}$); $S_{Au}{}^b$: gold surface area, HRTEM ($m^2\,g^{-1}$); D_{Au}: gold dispersion, HRTEM; n.m.: not measured.

C_2H_2 or C_2H_4 adsorption for 1 h (40 mL min^{-1}), followed by purging with He for 30 min and increasing the temperature to 500 °C, with a heating ramp of 10 °C min^{-1}.

2.3. Catalytic activity measurements

C_2H_2 hydrogenation was carried out in a lab-scale fixed bed reactor in which typically 0.15 g of catalyst was loaded. The standard reactivation procedure consisted of *in situ* heating the catalyst to 300 °C for 1 h under a H_2 flow (catalyst reduction). Alternatively, for Au/Al_2O_3 and $Au/CeO_x/Al_2O_3$ the hydrogen was replaced by O_2, in order to study the influence of the reactivation procedure. The feed gases were controlled by mass flow controllers (Bronkhorst) and set to a total flow of 40 mL min^{-1}. Diluted C_2H_2 and H_2 (4 vol% in He) were used to study the hydrogenation of acetylene. The reactant ratio was $C_2H_2/H_2 = 1/2$. The outlet gas concentration was on-line analysed by a gas chromatograph (Interscience Compact GC) equipped with FID (flame ionisation detector) and TCD (thermal conductivity detector), using two different columns: Molsieve 5 Å and Poraplot Q. Data analysis was performed using EzChrom software.

Typically the reactant mixture was stabilized for at least 30 min at room temperature. Afterwards the reaction temperature was ramped in steps of 20 °C, with a heating rate of 5 °C min^{-1} from room temperature to 250 °C. At each reaction temperature, the reaction was followed for 3 h in order to assess the deactivation of the catalyst.

The selective catalytic reduction (SCR) of acetylene in the presence of ethylene was performed in a similar manner as the hydrogenation of C_2H_2, using a reactant ratio of $C_2H_2/C_2H_4/H_2 = 1/1/2$. In addition, the direct hydrogenation of ethylene was also studied for a better understanding of the hydrogenation of C_2H_2 and C_2H_4 using a reactant ratio $C_2H_4/H_2 = 1/2$.

3. Results and discussion

3.1. Catalyst characterization

The average Au particle size as determined by XRD ranges from 4.3 nm, for un-promoted Au/Al_2O_3, to below the detection limit of XRD, when various additives are used (see Table 1). The metallic surface area based on the XRD results (see Table 1), was calculated by assuming that the gold particles are hemispherical in shape with the flat side on the support, according to the following formula:

$$S_{Au} = \frac{50,000W}{\rho d} \quad (1)$$

where W corresponds to the gold loading, ρ is the density of gold (19.3 $cm^3 g^{-1}$) and d is the diameter of gold particles as determined by XRD (Å) [19].

Since the size of the Au particles for the promoted catalysts was below the detection limit of the XRD (~3 nm), a further investigation of some of the Au-based catalysts by means of HRTEM was needed. The average Au particle size as determined by HRTEM is summarized in Table 1. In addition, Fig. 1 compares the particle size distribution of Au/Al_2O_3, $Au/CeO_x/Al_2O_3$ and $Au/BaO/Al_2O_3$. There is a significant difference concerning the particle size distribution of the samples with or without additive. The growth of the gold particles at the expense of the smaller Au crystallites found for Au/Al_2O_3 is prevented in the presence of the additives. In addition, we have observed by means of HRTEM and EDX (energy dispersive X-ray spectroscopy) that small gold nanoparticles preferentially nucleate on the additive-rich patches, which is highly important for the catalytic activity (see below), causing a stronger interaction of the Au nanoparticles with the support and a higher resistance to sintering.

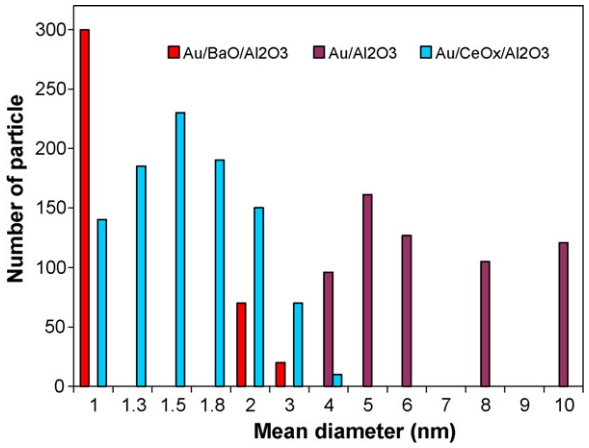

Fig. 1. Particle size distribution as determined by HRTEM for Au/Al_2O_3, $Au/BaO/Al_2O$ and $Au/CeO_x/Al_2O_3$.

The HRTEM micrographs of $Au/CeO_x/Al_2O_3$ and $Au/Li_2O/CeO_x/Al_2O_3$ are presented in Fig. 2a and b. Fig. 2a shows the well-resolved, high-resolution fingerprint of an Au particle that exhibits the (1 1 1) reflection, while Fig. 2b illustrates an example of a high-resolution TEM micrograph used to estimate the Au particle size distribution.

The results obtained by HRTEM have been also used to estimate the metallic surface area of some of the catalysts (see Table 1). According to the data presented in Table 1, the metallic surface area based on HRTEM data varies between 1.5 $m^2 g^{-1}$ (Au/Al_2O_3) and 7.1 $m^2 g^{-1}$ ($Au/CeO_x/Al_2O_3$). The differences between the values of the gold surface area determined by HRTEM and XRD may be related to the experimental limitations of each technique. However, it should be emphasized that both techniques are not completely suitable for this type of determination and that the results may be considered only as a relative measure of the metallic surface area of the catalysts. A very high dispersion (above 50%) was estimated for promoted Au-based catalysts (viz. $Au/CeO_x/Al_2O_3$ and $Au/BaO/Al_2O_3$), which considerably exceeds the estimated dispersion of Au/Al_2O_3 (11.5%).

3.2. C_2H_2 hydrogenation in the absence of C_2H_4

3.2.1. C_2H_2 hydrogenation in the absence of C_2H_4: effect of additives and Au particles size on the catalytic performance of Au/Al_2O_3

The reference catalyst Au/Al_2O_3 was first tested in C_2H_2 hydrogenation. The results are shown in Fig. 3. The reaction was performed using stoichiometric amounts of hydrogen for full conversion of C_2H_2 to C_2H_6 since a large concentration of hydrogen is not feasible for industry. As can be seen in Fig. 3, the acetylene conversion over Au/Al_2O_3 became significant at temperatures above 100 °C and it reached a 70% conversion at the maximum reaction temperature used in this study, viz. 250 °C. Very interestingly, the selectivity was 100% to C_2H_4 over the whole temperature range studied. We used a maximum reaction temperature of 250 °C because Pd-based catalysts are highly active in acetylene hydrogenation at temperatures that do not exceed 100–120 °C. Therefore, other types of catalysts that should compete with Pd-based catalysts should display a high catalytic activity in this temperature range. The results are comparable with earlier results published by Jia et al. [13] for Au/Al_2O_3, using the same reactant ratio $C_2H_2/H_2 = 1/2$ in batch mode. Those authors reported a similar reaction temperature and 100% selectivity towards C_2H_4.

The catalytic performance of the promoted Au-based catalysts is also shown in Fig. 3. We have been using the same additives

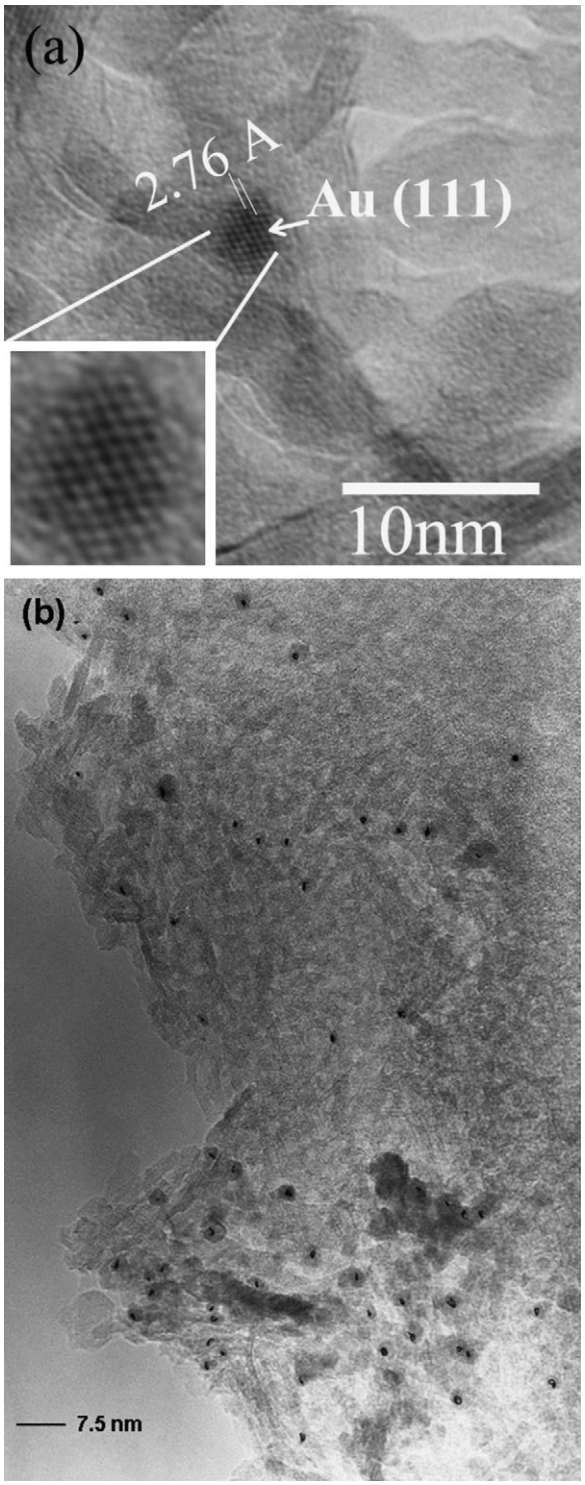

Fig. 2. HRTEM image of $Au/CeO_x/Al_2O_3$ (a), HRTEM image of $Au/Li_2O/CeO_x/Al_2O_3$ (b).

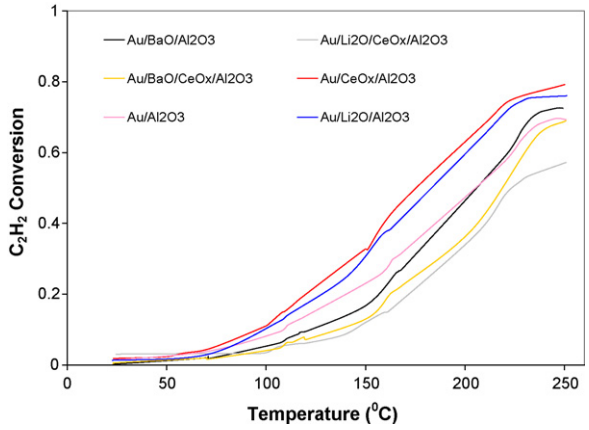

Fig. 3. C_2H_2 conversion versus temperature during C_2H_2 hydrogenation in the absence of C_2H_4. Reaction conditions: 0.15 g catalyst, 40 ml min^{-1} total feed, $C_2H_2/H_2 = 1/2$.

that in the past proved to promote the catalytic performance of Au/Al_2O_3 in various oxidation reactions studied in our laboratory [19–25]. According to the plots shown in Fig. 3, the best promoter effect was obtained with ceria and lithia. The fact that lithia has a promotion effect on the performance of Au/Al_2O_3 can be at least partly explained by the fact that acetylene is an acidic molecule and Li_2O has a basic character. The positive effect of ceria on the catalytic activity of Au/Al_2O_3 can only partly be attributed to basic character of ceria, while the well-known oxygen storage capacity of ceria could eventually drive the reaction into an opposite direction and make $Au/CeO_x/Al_2O_3$ an inactive catalyst. However, Au/CeO_2 was previously shown to be active in the hydrogenation of C_2H_2 under very large excess of hydrogen [16]. Other metal oxides that have been added to Au/Al_2O_3 had a less pronounced promoting effect as compared with ceria or lithia (see Fig. 3). It is worth to mention that all the catalysts displayed 100% selectivity to C_2H_4, without any trace formation of C_2H_6 (as was reported for Pd-based catalysts [3,7]) or methane and ethane, as was reported for other Au-based catalysts [16,17].

Table 2 summarizes the $T_{50\%}$ (the temperature needed to reach 50% C_2H_2 conversion), the specific reaction rate, r (defined as the number of C_2H_2 moles converted per number of Au moles and second) calculated at 110 °C and the apparent activation energy, E_a. The variation of r is a better way to compare the catalytic performance, including results obtained in other laboratories, since it is directly related to the nominal Au loading and reactant feed. The variation of r is consistent with the data shown in Fig. 3, Tables 1 and 2, and indicates, also when the data are presented in terms of C_2H_2 converted over the Au present in the sample, that the best results are obtained with $Au/CeO_x/Al_2O_3$, followed by $Au/Li_2O/Al_2O_3$. It is expected, based on the results published for Pd-based catalysts [1,3,14,26] and also on the study of Azizi et al. [16] that an increase of the H_2 concentration in the reactant mixture would drastically affect the reaction rate (i.e., by increasing it), especially when the rate determining step for this reaction is hydrogen activation.

As listed in Table 2, the apparent activation energy, calculated for a C_2H_2 conversion below 20%, varies between 28 kJ mol^{-1} (Au/Al_2O_3) and 37 kJ mol^{-1} ($Au/BaO/Al_2O_3$). It was previously reported that Pd-based catalyst showed an E_a around 38 kJ mol^{-1} [27], while apparent activation energy of 34 kJ mol^{-1} for Au/Al_2O_3 [13] and 37 kJ mol^{-1} Au/CeO_2 [16] have also been reported. The small variation in the apparent activation energy between unpromoted Au/Al_2O_3 and Au/Al_2O_3 promoted with various metal oxides points to the conclusion that the presence of the promoters do not open additional reaction pathways that would significantly affect the apparent activation energy, as compared with the reference catalyst.

A general statement valid for all oxidation reactions that employ Au as a catalyst is that the size of the Au particles is crucial in order to obtain an active Au-based catalyst [10,12,28]. The reaction between oxygen and hydrogen, on the other side, has been reported as a structure insensitive reaction [29]. When one tries to correlate the results presented in Tables 1 and 2 and Fig. 3, a straightforward correlation between the catalytic performance and size of the Au particles is not found. There is some depen-

Table 2
The temperature of 50% C_2H_2 conversion in the absence and in the presence of C_2H_4, the specific reaction rate calculated at 110 °C and the apparent activation energy.

Catalyst	$T^1_{50\%}$ (°C)	$r^1 \times 10^3$ ($mol_{C_2H_2}\ mol_{Au}^{-1}\ s^{-1}$)	E^1_a (kJ mol^{-1})	$T^2_{50\%}$ (°C)	$r^2 \times 10^3$ ($mol_{C_2H_2}\ mol_{Au}^{-1}\ s^{-1}$)	E^2_a (kJ mol^{-1})
Au/Al_2O_3	203	1.64	28 ± 2	227	1.78	42.1 ± 2
$Au/Li_2O/Al_2O_3$	181	2.06	29 ± 1	197	1.6	43.5 ± 1
$Au/BaO/Al_2O_3$	203	1.1	37 ± 1	220	0.9	42.4 ± 1
$Au/CeO_x/Al_2O_3$	172	2.5	32 ± 2	197	1.41	32.7 ± 2
$Au/Li_2O/CeO_x/Al_2O_3$	222	0.8	32 ± 1	245	0.6	37.9 ± 3
$Au/BaO/CeO_x/Al_2O_3$	218	0.94	29 ± 2	212	0.9	34.8 ± 2

$T^1_{50\%}$: temperature of 50% C_2H_2 conversion, $C_2H_2 + H_2$, r^1: specific reaction rate, $C_2H_2 + H_2$, E^1_a: apparent activation energy, $C_2H_2 + H_2$, $T^2_{50\%}$: temperature of 50% C_2H_2 conversion, $C_2H_2 + C_2H_4 + H_2$, r^2: specific reaction rate, $C_2H_2 + C_2H_4 + H_2$, E^2_a: apparent activation energy, $C_2H_2 + C_2H_4 + H_2$.

dence of the catalytic performance on the size of the Au particles, but a general trend is difficult to find, since $Au/CeO_x/Al_2O_3$, with a very high Au dispersion and very small Au particles (TEM and XRD) is highly active, but other catalysts such as $Au/BaO/Al_2O_3$, $Au/BaO/CeO_x/Al_2O_3$ or $Au/Li_2O/CeO_x/Al_2O_3$, having a comparable dispersion and mean size of the Au particles as $Au/CeO_x/Al_2O_3$, do not show a high performance in C_2H_2 hydrogenation.

In order to gain a better understanding concerning the influence of the size of the Au particles on the C_2H_2 conversion, we performed an additional hydrogenation test with catalysts that were (on purpose) heat-treated at high temperature (550 °C) for an extended period of time (8 h) in order to obtain Au-based catalysts with large Au particles (Table 1). The results are presented in Fig. 4. The mean diameter of the Au particles for the heat-treated samples, as determined by XRD (Table 1) ranges from 6.4 nm ($Au/Li_2O/Al_2O_3$) to 8.1 nm ($Au/BaO/CeO_x/Al_2O_3$). The results clearly indicate that for the same catalyst, the presence of larger Au particles have a strong, negative influence on the catalytic performance. The sample least affected by heat treatment, i.e., suffering from growing Au particles, appears to be $Au/Li_2O/Al_2O_3$ (Fig. 4), followed by Au/Al_2O_3 and $Au/CeO_x/Al_2O_3$. These data clearly show that over Au-based catalysts the hydrogenation of C_2H_2 is a structure-sensitive reaction and the size of the Au particles is very important: smaller Au particles lead to higher catalytic performance. Our results are complementary to what was already published by Jia et al. [13], where the authors state that the best catalytic performance for Au/Al_2O_3 is obtained with Au particles around 3 nm. Our data show that the catalytic performance of the Au-based catalysts can be further improved by using Au particles smaller than 3 nm. In addition, the data presented in this paper also show that the identity of the additives can play an important role.

3.2.2. *Catalytic activity of Au-based catalysts in C_2H_2 hydrogenation with time on stream, deactivation and regeneration*

A general characteristic of all the catalysts that show activity in C_2H_2 hydrogenation is that they suffer severe deactivation with time on stream. The catalysts based on Pd were extensively studied and several models have been proposed that can explain the deactivation phenomena [7]. Some authors claim that during reaction a lot of "green oil" is formed, which is partly related to the identity of the catalyst and reaction temperature [4]. On Au/CeO_2, Azizi et al. [16] found that CH_4 and C_2H_6 are detected in the gas phase, together with C_2H_4, while some other species are adsorbed on the surface.

The catalysts tested in this study also deactivate with time on stream and we were interested to study the nature of this deactivation phenomena, i.e., if it is reversible, due to some C deposits on the surface, or it is irreversible, due to, for example, Au sintering. In the next step we were interested to restore the catalytic performance. In order to accomplish this we applied a "de-coking" procedure, which is basically burning off in oxygen all the species adsorbed on the surface of the catalyst. The maximum temperature used during "de-coking" was 500 °C. We have then undertaken two actions: we monitored the species which were desorbing during "de-coking" (Fig. 5) and we tested again the catalysts in C_2H_2 hydrogenation (see Fig. 6).

A closer look to the CO_2 desorption peaks as depicted in Fig. 5 allows us to make some correlations between the CO_2 desorption peak, its intensity and the catalytic performance. The number of desorption peaks could give information about the nature of the C deposits and their location. CO_2 is formed below 300 °C on $Au/Li_2O/CeO_x/Al_2O_3$, $Au/CeO_x/Al_2O_3$ and $Au/BaO/CeO_x/Al_2O_3$. Above 350 °C we found CO_2 formation on Au/Al_2O_3 and $Au/Li_2O/Al_2O_3$ catalysts. Another interesting feature

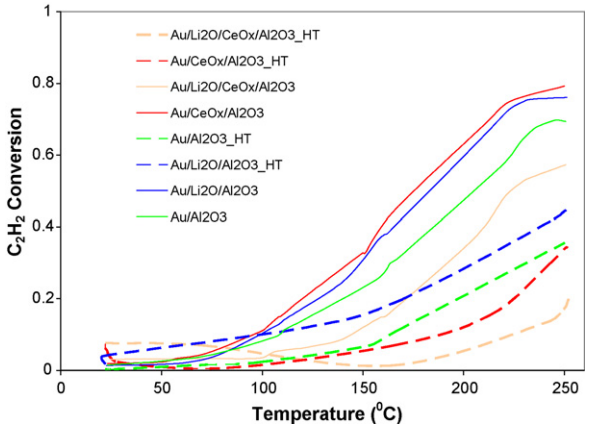

Fig. 4. Comparison of the catalytic performance during C_2H_2 hydrogenation for the as-prepared catalysts and the high temperature treated catalysts (sintered). The plot shows C_2H_2 conversion versus temperature in the absence of C_2H_4. Reaction conditions: 0.15 g catalyst, 40 mL min^{-1} reactant feed, $C_2H_2/H_2 = ½$, "HT" – high temperature treatment.

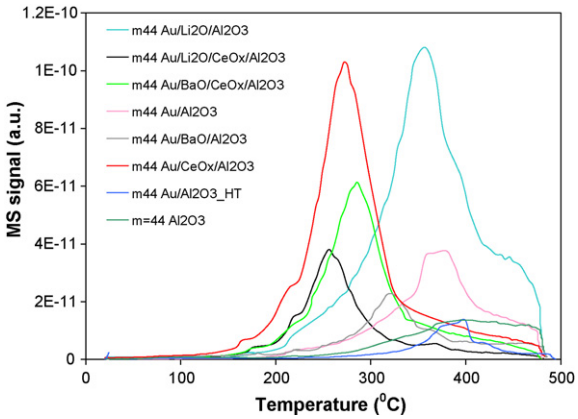

Fig. 5. CO_2 formation during de-coking of the catalysts after C_2H_2 hydrogenation in the absence of C_2H_4. "m44" corresponds to the CO_2 signal as measured by the mass spectrometer (MS) during de-coking (oxygen temperature pre-treatment), HT"-high temperature treatment.

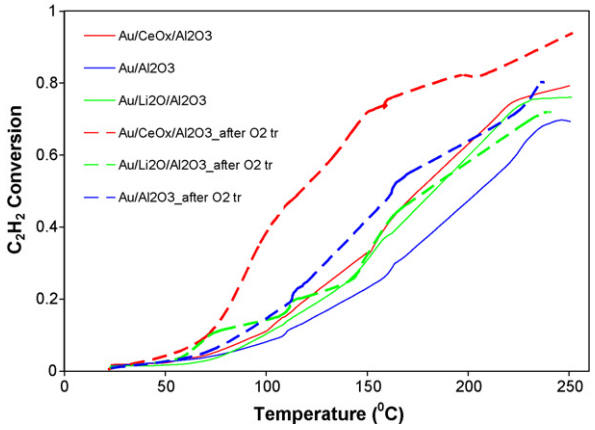

Fig. 6. Comparison of the C_2H_2 conversion versus temperature of the as-prepared catalysts and the same catalysts after they have been de-coked (O_2 temperature treatment). Reaction conditions: 0.15 g catalyst, 40 mL min^{-1} reactant feed, $C_2H_2/H_2 = 1/2$. "Catalyst_after O2 tr" refers to a catalyst tested after an oxygen pre-treatment, also referred in text as de-coking.

is the amount of CO_2 desorbed from the catalysts, taking into account that all the experiments were conducted with the same amount of catalyst. The CO_2 peak is considerably higher for catalysts such as $Au/CeO_x/Al_2O_3$ and $Au/Li_2O/Al_2O_3$, pointing to a direct correlation between the CO_2 peak area and the catalytic performance, eventually correlated with the promoter's identity. The area of the desorption peak is almost double for $Au/Li_2O/Al_2O_3$, as compared with $Au/CeO_x/Al_2O_3$.

There are not so many data available concerning this kind of studies carried out over Au-based catalysts. However, there are some reports concerning the CO_2 desorption from Au/CeO_2 [16] and Au/SiO_2 and Au/TiO_2 [17]. Using five times more hydrogen than C_2H_2 in the gas stream and aging the catalyst at 210 °C for 6 h, a single CO_2 desorption peak around 243 °C was found on Au/CeO_2 [16]. If the C_2H_2 hydrogenation was performed between 210 and 400 °C, three CO_2 desorption peaks were found, at 245, 340 and 440 °C, respectively. The authors assigned these desorption peaks to unstructured carbon, or trapped hydrocarbons (lowest desorption peak), amorphous coke (340 °C) and acidic carbon (highest desorption temperature). Performing de-coking of Au/TiO_2 or Au/SiO_2, Sarkany found one main desorption peak centred at 227° or 277°, depending on the support, accompanied by eventually some small shoulders at 277° or 327 °C [17]. No clear assignment of the coke identity was made. Other authors observed on Pd-based catalysts also three desorption peaks which were assigned to: hydrocarbons located in the pores (low temperature peak), green oil in the vicinity of the Pd (300–500 °C) and green oil produced on the support without influence of the Pd [7]. Ni/SiO_2 showed two desorption peaks after de-coking, one at 320 °C, assigned to filamentous carbon, and a second one at higher temperatures (400 °C), assigned to amorphous coke [30]. The same authors found for Ni/SiO_2-Al_2O_3 a third peak, located at 475 °C, attributed to acidic coke. It is clear that the reported results are quite different and the CO_2 formation depends on several factors, such as active metal, support identity and reaction temperature. We believe that an additional factor that influences the CO_2 desorption range is directly related to the size of the Au particles. The aim of this article was not to study the nature of the carbonaceous deposits that evolved from the various gold surfaces after de-coking experiments, but based on our results we can tentatively assign the desorption peak at 250 °C to carbon species coming from weakly adsorbed acetylene, while the second desorption peak is related to C fragments that desorb at higher temperatures (~370 °C) and are stronger bound to the support.

There are a number of reasons that support our assumptions: although the CO_2 desorption plots for $Au/CeO_x/Al_2O_3$ and $Au/Li_2O/Al_2O_3$ are quite different, the catalysts exhibit a very similar performance in the hydrogenation of C_2H_2. Therefore the low and high temperature peaks are, most likely, not due to carbonaceous deposits desorbing from different locations on the surface of the catalyst, but are rather an Au particle size effect. The low temperature CO_2 desorption peak may be related to a higher abundance of low-coordinated Au sites (edges, kinks and corners) of $Au/CeO_x/Al_2O_3$, which are more reactive at lower temperature, compared with other C fragments which would be burned off at higher temperatures and are related to C_2H_2 adsorbed on larger Au particles ($Au/Li_2O/Al_2O_3$) which have relatively less low-coordinated sites.

It is expected that a higher metallic dispersion would cause a smaller amount of coke than a lower metallic dispersion surface. The temperature of the CO_2 peaks for the other catalysts are in line with the variation of the size of the Au particles. The small variations in the desorption maximum are most likely related to an additional influence of the promoter's nature, basic or acid. Additional proof to support the above mentioned model is shown in Fig. 5 in terms of the CO_2 desorption peak of Au/Al_2O_3 that was treated for an extended period of time at high temperature (550 °C) and the Au particles are significantly larger (7.1 nm) than for the same sample that was calcined at 300 °C. These data support our assumption that the CO_2 desorption temperature is mainly, but not only, related to the size of the Au particles and their dispersion.

The experimental findings, as depicted in Fig. 6, were also very interesting: all the catalysts showed superior activity after the "de-coking" procedure, suggesting two conclusions: firstly, the catalytic performance is easily restored after an oxygen treatment, and secondly, the catalysts became even more active as compared with the catalysts shown in Fig. 3, where a reductive treatment was applied prior to reaction. The catalytic performance of $Au/CeO_x/Al_2O_3$ and Au/Al_2O_3 were strongly influenced by the O_2 treatment. It has to be noted that the selectivity during hydrogenation was still 100% to C_2H_4.

The fact that the catalytic performance could be restored after de-coking indicates that the loss of the catalytic performance in time is due to C deposited on the surface and this is easily burned off during an oxygen treatment and the deactivation is not due to sintering of Au particles. The explanation for the improved catalytic activity after burning off the coke is not straight forward. There could be at least two reasons of the improved catalytic activity during de-coking, i.e., either a change in the chemical state of the Au, which could become partly oxidized after de-coking, or a change in the chemical state of CeO_x, with Ce^{4+} being more active than Ce^{3+}. Some additional experiments were performed. The results are shown in Fig. 7 where Au/Al_2O_3 and $Au/CeO_x/Al_2O_3$ are compared with catalysts that are either reactivated in O_2 ($Au/CeO_x/Al_2O_3$_O_2 react and Au/Al_2O_3_O_2 react) prior to hydrogenation of C_2H_2 (in order to distinguish between the effect of Ce^{4+} and Ce^{3+}) or dried, viz. $Au/CeO_x/Al_2O_3$ dry, which contains both Ce^{4+} and Au^{3+}. The results clearly show that Ce^{4+} is the active species, since $Au/CeO_x/Al_2O_3$_O_2, consisting of mainly Au^0 and Ce^{4+}, is more active than $Au/CeO_x/Al_2O_3$, a catalyst reduced under hydrogen prior to reaction and which contains mainly Au^0 and Ce^{3+} [25]. These results also explain why the catalysts after de-coking (which is similar to oxygen pre-treatment) are more active than the ones that were reduced prior to reaction (Fig. 3). The results also show that Au^{3+} does not show significant activity, since $Au/CeO_x/Al_2O_3$ dry, containing mainly Au^{3+} and Ce^{4+}, does not show significant activity and the presence of the metallic Au is more important, compared with Au^{3+}. After de-coking, the Au surface undergoes probably some reconstruction and/or rearrangement that leads to a large improvement in the catalytic performance. The reason why

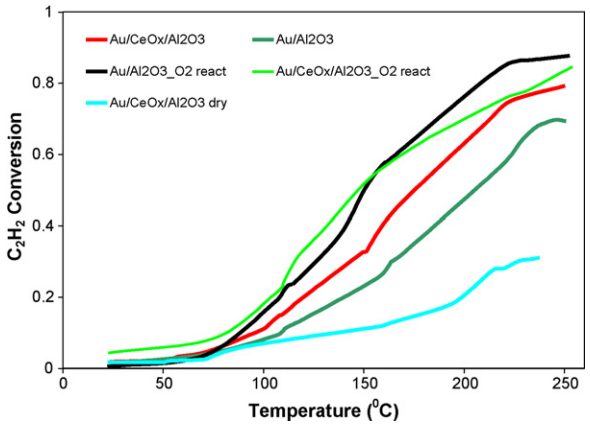

Fig. 7. The effect of pre-treatment on the Au/Al_2O_3 and $Au/CeO_x/Al_2O_3$ catalysts for the C_2H_2 hydrogenation in the absence of C_2H_4. "Catalyst_O2 react" refers to a catalyst tested after an oxygen pre-treatment, "catalyst dry" refers to a catalyst tested immediately after preparation, when the only thermal treatment was drying in air at 80 °C for 16 h. Note that reactivation of the catalysts using O_2 pre-treatment is applied to the fresh catalysts, while oxygen temperature treatment or de-coking is used to restore the catalytic performance of the spent catalysts.

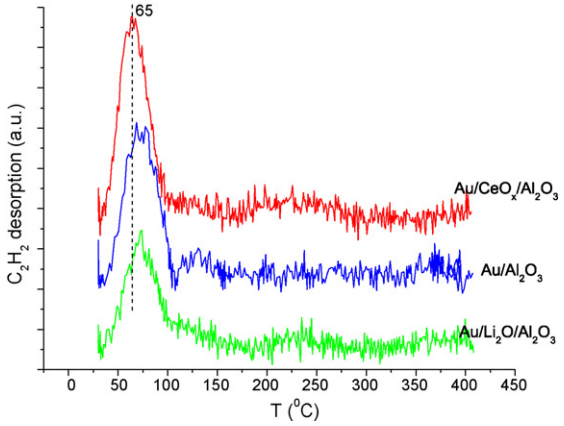

Fig. 9. C_2H_2 and C_2H_4 desorption from selected Au-based catalysts. Experimental conditions: 0.2 g catalyst, C_2H_2 or C_2H_4 adsorption for 1 h (40 mL min^{-1}), purge with He for 30 min and heat-up in He to 550 °C with 10 °C min^{-1}.

an oxidized ceria surface is more active towards hydrogen activation and C_2H_2 reduction is not completely clear. However, there are some reports that claim that Ce^{4+} can chemisorb large amounts of hydrogen, and the adsorption/desorption of H_2 is very sensitive to the presence of a dispersed metal as well as the pre-treatment of the catalyst [31,32].

3.3. Selective catalytic reduction of C_2H_2 in the presence of C_2H_4

After performing various studies in order to understand the effect of the size of the Au particles, the influence of different promoters, ways of activation of the catalysts in the hydrogenation of C_2H_2, we focused on the selective hydrogenation of C_2H_2 in the presence of C_2H_4. The results are presented in Fig. 8 in terms of C_2H_2 conversion versus temperature in the presence and the absence of C_2H_4. In addition, Table 2 summarizes the $T_{50\%}$, the temperature needed to convert 50% of C_2H_2, the specific reaction rate r calculated at 110 °C and the apparent activation energy estimated for conversion of C_2H_2 below 20%. One general characteristic of all the catalysts tested in the SCR of C_2H_2 is that their performance is slightly shifted towards higher temperatures, as compared with C_2H_2 hydrogenation in the absence of C_2H_4. The same conclusion can be drawn from the data presented in Table 2. $Au/CeO_x/Al_2O_3$

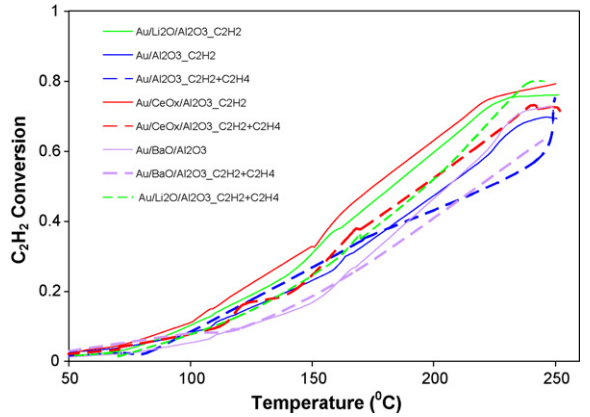

Fig. 8. C_2H_2 conversion versus temperature during SCR of C_2H_2 in the presence of C_2H_4. Reaction conditions: 0.15 g catalyst, 40 mL min^{-1} reaction feed, $C_2H_2/H_2/C_2H_4 = 1/2/1$.

still performs the best, and Au/Al_2O_3 is very similar in its performance, if one compares the catalysts only on the basis of plots depicted in Fig. 8. However, the data shown in Table 2 shows that, depending on the temperature range, i.e., around 110 °C, Au/Al_2O_3 performs slightly better than $Au/CeO_x/Al_2O_3$. However, the lowest apparent activation energy is found for $Au/CeO_x/Al_2O_3$. Similar with the hydrogenation of C_2H_2 in the absence of C_2H_4, the differences between E_a for all the tested catalysts do not point to new reaction pathways in the presence of the promoters. It is very important to mention that the $S_{C_2H_4}$ is still 100% over the whole temperature range studied. This very important result shows the real potential of Au-based catalysts in SCR of C_2H_2. It is expected that increasing the partial pressure of H_2 would have a positive influence on the conversion of C_2H_2, without affecting the selectivity towards C_2H_4. This conclusion is based on some additional work we have performed which is described below. Firstly, we also studied the hydrogenation of C_2H_4 in the absence of C_2H_2 and we found that all the catalysts are completely inactive over the whole temperature range studied, unlike Pd-based catalysts which easily hydrogenate C_2H_4 to C_2H_6. Secondly, we performed co-adsorption studies of C_2H_2 and C_2H_4 over the most active Au-based catalysts and monitored the desorption products. The results are shown in Fig. 9. It was very interesting to observe that if both C_2H_2 and C_2H_4 were fed over the catalysts for 1 h at room temperature, the only desorption product when the temperature is ramped to 500 °C is C_2H_2, with one major peak below 100 °C. The areas of the C_2H_2 desorption peaks as shown in Fig. 9 are in line with the reactivity of the catalysts in SCR of C_2H_2.

The key to 100% C_2H_4 selectivity when both C_2H_2 and C_2H_4 are hydrogenated is the absence of C_2H_4 adsorbed on the Au surface. It is clear that the adsorption of the triple bond is preferred over the double bond and during SCR of C_2H_2 the two hydrocarbons do not compete for the same adsorption sites.

The results also point to the conclusion that the rate determining step during either C_2H_2 hydrogenation or SCR of C_2H_2 is the activation of hydrogen, most likely with the hydrocarbon associatively adsorbed on the Au surface. It was already shown that in the hydrogenation of C_2H_2 a higher concentration of hydrogen improves the conversion of C_2H_2 [16]. It is likely that also SCR of C_2H_2 will benefit from a higher concentration of H_2 in terms of C_2H_2 hydrogenation and most likely the selectivity to C_2H_4 would not be significantly affected. This assumption is based on the TPD results (Fig. 9) that clearly show that C_2H_4 does not stick to the Au surface in a detectable amount and most likely it desorbs very fast after it is formed as a hydrogenation product during SCR of C_2H_2.

4. Conclusions

We have undertaken an extensive study of C_2H_2 hydrogenation in the presence and the absence of C_2H_4 over Au-based catalysts. A number of parameters were varied: Au particle size, pre-treatment conditions, nature of the additives. The deactivation of the catalysts during $C_2H_2 + H_2$ was also studied in detail.

Our findings are summarized below:

- The selectivity to C_2H_4 is 100% for a reaction temperature below 250 °C.
- The size of the Au particles is a very important parameter, Au particles below 3 nm are enhancing C_2H_2 conversion both in the absence and in the presence of C_2H_4, without affecting the selectivity to C_2H_4.
- Au° is the active species during hydrogenation.
- Ce^{4+} proved to be more active than Ce^{3+}.
- The presence of Li_2O is beneficial for higher C_2H_2 conversion. Both BaO and Li_2O do not affect the selectivity to C_2H_4.
- An oxygen pre-treatment helps in activating C_2H_2 and H_2 better than a pre-treatment in hydrogen.
- The deactivation during C_2H_2 hydrogenation is a reversible process and is due to accumulation of C deposits as a result of C_2H_2 adsorption on different active Au sites. These deposits can be easily burned off by a thermal treatment in oxygen.
- The selectivity towards C_2H_4 is 100% also when C_2H_4 is present in the gas stream, although the C_2H_2 hydrogenation temperature is shifted to slightly higher temperatures, as compared to hydrogenation of C_2H_2 in the absence of C_2H_4.

Acknowledgment

The Netherlands Organization for Scientific research, NWO (Grants NWO/CW 99037 and NWO #047.015.003) is gratefully acknowledged for financial support.

References

[1] Y.H. Park, G.L. Price, Ind. Eng. Chem. Res. 31 (1992) 469.
[2] V. Ponec, G.C. Bond, Stud. Surf. Sci. Catal. 95 (1995) 491.
[3] J. Panpranot, K. Kontapakdee, P. Praserthdam, J. Phys. Chem. B 110 (2006) 8019.
[4] I.Y. Ahn, J.H. Lee, S.S. Kum, S.H. Moon, Catal. Today 123 (2007) 151.
[5] C. Shi, B.W.-L. Jang, Ind. Eng. Chem. Res. 45 (2006) 5879.
[6] W. Huang, J.R. McCormick, R.F. Lobo, J.G. Chen, J. Catal. 246 (2007) 40.
[7] I.Y. Ahn, W.J. Kim, S.H. Moon, Appl. Catal. A: Gen. 308 (2006) 75.
[8] W. Huang, W. Pyrz, R.F. Lobo, J.G. Chen, Appl. Catal. A: Gen. 333 (2007) 254.
[9] M. Haruta, T. Kobayashi, N. Yamada, Chem. Lett. 2 (1987) 405.
[10] G. Bond, C. Louis, D.T. Thompson, Catalysis by Gold, Imperial College Press, 2006.
[11] P. Claus, Appl. Catal. A 291 (2005) 222.
[12] G.C. Bond, D.T. Thompson, Catal. Rev. Sci. Eng. 41 (1999) 319.
[13] J. Jia, K. Haraki, J.N. Kondo, K. Domen, K. Tamaru, J. Phys. Chem. B 104 (2000) 1153.
[14] A. Sárkány, A. Horváth, A. Beck, Appl. Catal. A: Gen. 229 (2002) 117.
[15] T.V. Choudhary, C. Sivadinarayana, A.K. Datye, D. Kumar, D.W. Goodman, Catal. Lett. 86 (2003) 1.
[16] Y. Azizi, C. Petit, V. Pitchon, J. Catal. 256 (2008) 338.
[17] A. Sárkány, React. Kinet. Catal. Lett. 96 (2009) 43.
[18] Y. Segura, N. López, J. Pérez-Ramírez, J. Catal. 247 (2007) 383.
[19] A.C. Gluhoi, Fundamental studies focused on understanding of gold catalysis, PhD thesis, Leiden University, Leiden, 2005, ISBN: 90-9019950-0.
[20] A.C. Gluhoi, N. Bogdanchikova, B.E. Nieuwenhuys, J. Catal. 229 (2005) 154.
[21] A.C. Gluhoi, N. Bogdanchikova, B.E. Nieuwenhuys, J. Catal. 232 (2005) 96.
[22] A.C. Gluhoi, M.A.P. Dekkers, B.E. Nieuwenhuys, J. Catal. 219 (2003) 197.
[23] A.C. Gluhoi, S.D. Lin, B.E. Nieuwenhuys, Catal. Today 90 (2004) 175.
[24] A.C. Gluhoi, B.E. Nieuwenhuys, Catal. Today 122 (2007) 226.
[25] A.C. Gluhoi, X. Tang, P. Marginean, B.E. Nieuwenhuys, Top. Catal. 39 (2006) 101.
[26] P. Praserthdam, B. Ngamsom, N. Bogdanchikova, S. Phatanasri, M. Pramotthana, Appl. Catal. A: Gen. 230 (2002) 41.
[27] H. Molero, B.F. Bartlett, W.T. Tysoe, J. Catal. 181 (1999) 49.
[28] M. Haruta, Catal. Today 36 (1997) 153.
[29] M. Haruta, N. Yamada, T. Kobayashi, S. Iijima, J. Catal. 115 (1989) 301.
[30] C. Guimon, A. Auroux, E. Romero, A. Monzon, Appl. Catal. A: Gen. 251 (2003) 199.
[31] S. Bernal, J.J. Calvino, G.A. Cifredo, J.M. Rodrigues-Izquierdo, V. Perrichon, A. Laachirt, J. Catal. 137 (1992) 1.
[32] S. Bernal, J.J. Calvino, G.A. Cifredo, J.M. Gatica, J.A.P. Omil, J.M. Pintado, J. Chem. Soc., Faraday Trans. 89 (1993) 3499.